Multiplexed Conformationally-Selective, Localized Gas-Phase Hydrogen Deuterium Exchange of Protein Ions Enabled by Transmission-Mode Electron Capture Dissociation

Ritu Chaturvedi[1†], Ian K. Webb*[1,2]

[1]Department of Chemistry and Chemical Biology, Indiana University Purdue University Indianapolis, Indianapolis, Indiana 46202, United States

[2]Center for Computational Biology and Bioinformatics, Indiana University School of Medicine, Indianapolis, Indiana 46202, United States

ABSTRACT: In this article, we present an approach for conformationally multiplexed localized hydrogen deuterium exchange (HDX) of gas-phase protein ions facilitated by ion mobility (IM) followed by electron capture dissociation (ECD). A quadrupole-ion mobility-time of flight instrument previously modified to enable ECD in transmission mode (without ion trapping) immediately following a mobility separation was further modified to allow for deuterated ammonia (ND_3) to be leaked in after *m/z* selection Collisional activation was minimized to prevent deuterium scrambling from giving structurally irrelevant results. This arrangement was demonstrated with the extensively studied protein folding models ubiquitin and cytochrome c. Ubiquitin was ionized from conditions that stabilize the native state and conditions that stabilize the partially-folded *A*-state. IM of deuterated ubiquitin 6^+ ions allowed the separation of more compact conformers from more extended conformers. ECD of the separated subpopulations revealed that the more extended (later arriving) conformers had significant, localized differences in the amount of HDX observed. The 5^+ charge state showed greater protection against HDX than the compact 6^+ conformer, and the 11^+ charge state, ionized from conditions that stabilize the *A*-state, showed much greater deuterium incorporation. The 7^+ ions of cytochrome c ionized from aqueous conditions showed greater HDX with exterior and more unstructured regions of the protein, while interior, structured regions, especially those involved in heme binding, were more protected against exchange. These results, as well as potential future methods and experiments, are discussed herein.

INTRODUCTION

As a result of the development of electrospray ionization (ESI),[1] mass spectrometry (MS), especially tandem mass spectrometry (MS/MS), has been used for studies of three-dimensional structure in proteins and other biomacromolecules.[2] The most popular approaches use either irreversible[3-4] or reversible labeling,[5] in native-like solution conditions or inside cells themselves.[6] Irreversible labeling is performed by covalent modification of the protein and includes both specific and non-specific labels. For example, n-hydroxysuccinimide (NHS) esters label lysines,[7] and by using various length linker groups between two NHS groups, covalent cross-linking experiments can be used to generate distance constraints between intra and intermolecular lysines.[8] Non-specific labels are often used in footprinting experiments, where the solvent accessible sites as well as binding sites can be determined (e.g., through photoactivated carbene and hydroxyl radical methods).[9-11] With these covalent approaches, the labels survive enzymatic digestion, allowing for the superior sensitivity of LC/MS/MS bottom-up proteomics to be used to identify labeled peptides.[12] These peptides are rolled up into their constituent proteins to determine which regions of the protein were labeled. The most widely-used reversible labeling approach is hydrogen deuterium exchange (HDX).[5] In protein HDX, labile, accessible hydrogens exchange with deuteriums in the solvent (typically amide backbone hydrogens in a D_2O solution). By quenching exchange with acid and cleavage with pepsin (trypsin is inactive in acidic solutions), back-exchange between the deuterated protein and solvent can be avoided.[13] The chromatographic separations are also run at reduced temperatures in order to help prevent back-exchange of the deuterons that have labeled the proteins with protons in the solvent. Due to the possibility of deuterium scrambling (i.e., deuterons mobilize and bind to new amide nitrogen atoms) by collisional heating, tandem mass spectrometry is not usually used in the bottom-up HDX workflow.[14] In these experiments, the extent of HDX is monitored, and by varying the labeling time, kinetic uptake information can be measured that reports on the dynamics of different regions of the protein and can be used to elucidate binding sites.[15] HDX is advantageous since it is universally applicable and does not cause label-induced structural changes that may occur with irreversible labeling, affecting the ability of multiple irreversible labels to accurately measure three-dimensional structure.[16]

† Current Address:
Institute of Organic Chemistry and Biochemistry of the Czech Academy of Sciences
Flemingovo náměstí 2
16610 Prague, Czech Republic

Another MS workflow growing in popularity for measuring three-dimensional structure of proteins is native MS.[17-19] In a native MS experiment, low micromolar concentrations of proteins solvated with a biologically realistic ionic strength of volatile salts (e.g., 200 mM ammonium acetate) are ionized via electrospray to stabilize native-like structures. Native mass spectrometry has been used, for example, to measure stoichiometries of protein-protein[20] and protein-ligand complexes,[21] evaluate heterogeneity of heavily modified proteins, such as antibodies and biotherapeutics,[22] and measure membrane proteins.[23] In many native MS experiments, the exact preservation of all aspects of solution structure is unnecessary as long as the overall mass of the native-like complex, its binding partners, and modifications is unaffected. However, a key aspect of the electrospray process is that ions are significantly cooled, kinetically trapping solution states that do not interconvert on the MS experimental timescale.[24] Ion mobility (IM) coupled to MS (IM/MS) has been used to successfully characterize three-dimensional structures of kinetically trapped solution states, taking advantage of the speed and sensitivity of the combined IM/MS approach. The mobilities of ions depend on the overall shape and size to charge ratio of the ions, enabling experimental determinations of collision cross sections (between the ions of interest and an inert drift gas) at low electric fields.[25] These cross sections can be predicted via computational approaches from modeled or measured atomistic structures, allowing the gas-phase and condensed-phase structures to be compared.[26] With sufficient resolution, IM/MS can be used to separate individual conformers or conformer families to allow for conformationally-selective measurements. Since the charge states generated by ESI correlate to the solvent accessible surface area (SASA) of proteins in solution,[27] a combined charge-selective (via *m/z* selection) and mobility-selective (via IM) approach is a rapid and powerful technique in structural biology. The exquisite selectivity of IM/MS/MS (or MS/IM/MS) measurements allows them to be uniquely capable of providing conformationally-selective structural measurements of heterogeneous and dynamic protein systems.[28]

To gain localized three-dimensional structural information, it is desirable to couple a labeling technique with structurally selective IM/tandem MS. To this end, approaches for covalent[29-31] and non-covalent[32] irreversible labeling in the gas-phase have been coupled with MS/IM/MS workflows. In addition, gas-phase HDX has been used in various mass analyzers[33-36] and ion optics[37-38] towards three-dimensional structural determination. HDX reagents are leaked into the ion optics of choice, and ions collide with reagents. The resulting ion/molecule reactions result in the exchange of hydrogens with deuteriums on the reagent. On the millisecond timescales of gas-phase HDX in intermediate pressure ion guides, labeling occurs with fast-exchanging sites. Instead of exchanging with amide backbone hydrogens, deuterons exchange with ionizing protons, N-terminus amine hydrogens, the acidic hydrogen at the C-terminus, and hydrogens bound to heteroatoms in residue side chains.[39] Deuterium scrambling during fragmentation, since there is no enzymatic digestion in these experiments to localize HDX, can be mitigated by not using any collisional activation but using electron-based fragmentation methods, like electron capture dissociation (ECD), which have been shown to greatly minimize scrambling.[40] Previous IM/tandem MS approaches to gas-phase HDX have utilized electron transfer dissociation (ETD) after labeling and prior to the ion mobility separation,[39] or after ion mobility separation.[41] ETD requires trapping of radical anionic reagents with the deuterated proteins and peptides, and thus, ETD performed after mobility selection requires narrow mobility windows to be consecutively selected and trapped to gain conformer specific localized HDX.[41] ETD performed before the IM separations prevents mobility selected localized HDX from being measured, since mobility separates fragments produced from the mixture of all conformers related to a particular charge state. In this work, we have developed a workflow for conducting ECD after mobility separation, using an electromagnetostatic cell[42] that allows for ECD without trapping the deuterated ions. Thus, HDX and ECD are multiplexed for the entire ion mobility arrival time distribution (ATD). Since the fragments of transmission-mode ECD are aligned with both charge state selection and mobility separation, our workflow gives us an added dimension of conformationally selectivity in HDX measurements without sacrificing the inherent speed of IM/time-of-flight MS measurements.[43]

EXPERIMENTAL SECTION

Reagents and Samples. Ubiquitin from bovine erythrocytes, cytochrome c from horse heart, ammonium acetate, and a 25 L cylinder of 99 atom% D ammonia-d3 (ND_3) were purchased from Sigma-Aldrich (St. Louis, MO). Methanol and formic acid were obtained from Fisher Scientific (Fairmont, NJ). Water was obtained from a Milli-Q Millipore A10 (Burlington, MA) water purification system at a resistivity of 18 MΩ-cm or greater. For denaturing conditions, ubiquitin was prepared at 10 mM in a mixture of 50/50 vol/vol solution of water/methanol and 0.1% formic acid, conditions favoring the partially unfolded A state in solution.[44] For aqueous, native-like conditions, ubiquitin and cytochrome c were dissolved in aqueous 200 mM ammonium acetate solutions for final protein concentrations of 10 μM.

Ion Mobility Mass Spectrometry and HDX. All experiments were performed on a modified Synapt G2-Si High Definition Mass Spectrometer (Waters Corporation, Wilmslow, U.K.), equipped with electron transfer dissociation (ETD), a NanoLockspray source, an external electrospray voltage control module (GAA Custom Electronics LLC, Kennewick, WA), and an ExD cell (e-MSion, Corvallis, OR). Instrumental details have been described previously.[29-32,42] The NanoLockspray source was used with proteins introduced by nanoelectrospray ionization (nESI) from a pulled borosilicate glass capillary (P97 Flaming/Brown Micropipette puller, Sutter Instrument Company, Novato, CA) with a platinum wire inserted through the distal end of the capillary held at a positive potential of ~1 kV. Various charge states of the proteins produced by nESI were mass selected in the quadrupole for reaction with ND_3 in the trap cell (Figure 1). Following HDX in the trap, ions were injected into the mobility cell, where they were separated by their gas-phase size/shape to charge ratios using a traveling wave at 40 V and a wave velocity of 1000 m/s. Ions exiting the mobility cell traversed the ExD cell, with a filament current of 2.5 amps producing approximately 3 eV electrons for ECD fragmentation. No collisional energy was applied. Fragments were mass analyzed in the time of flight (TOF) in resolution mode (nominal resolving power of 20,000).

The modification of a Synapt Q-IM-TOF to enable gas-phase HDX with *m/z* selected ions in the trap cell has been previously reported.[45] Briefly, the 1/8" gas line into the trap cell was teed into with a Swagelok tee and shutoff valve (Swagelok, Indianapolis, IN). The pressure of ammonia gas was regulated via a corrosive gas lecture

bottle regulator (Matheson Tri-Gas, Joliet, IL), a Swagelok metering valve, and restriction capillary comprised of three 50 cm of PEEKSil 1/16" OD, 100 μm ID capillaries (Sigma Aldrich) connected to the 1/8" tubing by Swagelok 1/8" to 1/16" and 1/16" to 1/16" unions. Enough gas was allowed into the system to increase the trap cell background pressure by 20 μbar with ETD (to deliver helium to the trap cell) and mobility modes enabled. No ETD was performed. The trap cell was operated with a trap traveling wave height of 1 V and velocity of 300 m/s to allow for adequate reaction time between the proteins and the ND_3 gas. Deuterated protein mass spectra were observed without significantly decreasing the sensitivity of the ion signal. Deuterated and non-deuterated proteins were measured and fragmented by ECD in triplicate, with the extents of deuteration for ECD fragments determined and manually validated through HDExaminer (Sierra Analytics, Modesto, CA) by calculating the weighted average of the isotope distributions of both the non-deuterated and deuterated fragments.

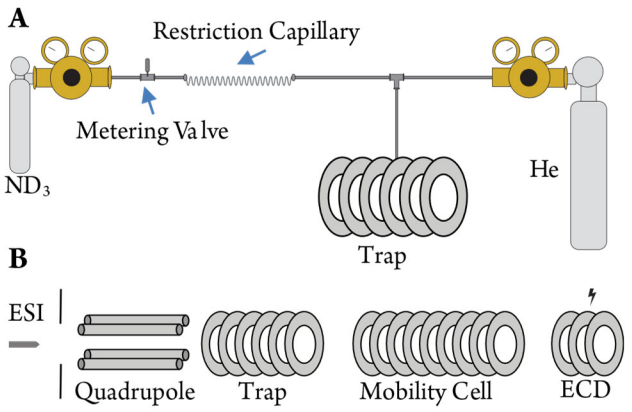

Figure 1. (A) Cartoon illustration of the in-trap gas-phase HDX setup. During gas-phase HDX, ND3 is leaked into the trap cell such that the background pressure increases by ~20 μbar (15 mtorr). (B) Protein charge states selected by their *m/z* react with ND3 in the trap cell, undergo mobility separation in the mobility cell, and are fragmented in the ExD cell. No collision energy was applied in any of the experiments.

RESULTS AND DISCUSSION

Residue Specific Deuterium Uptake for Ubiquitin 6^+. The protein ubiquitin has previously been used as model for in source and gas-phase HDX.[39, 46-47] As such, we began our characterization of in-trap HDX with on-the-fly ECD fragmentation by examining various charge states of ubiquitin produced by nESI from aqueous ammonium acetate and water/methanol/acid solutions. For example, isolation of the 6^+ charge state by the quadrupole with and without the addition of ND_3 in the trap cell is shown in Figure 2. In Figure 2A, the isotopic distributions of intact ubiquitin 6^+ with and without HDX are displayed. Under the conditions we are using (i.e., ~20 μbar partial pressure ND_3, trap traveling wave height 1 V, 300 m/s), the *m/z* ratio increases by 6.8696 from being centered at 1428.5228 *m/z* to 1435.3924 *m/z*. This indicates the incorporation of, on average, approximately 41 deuteriums. The 5^+ charge state, generated by nESI from aqueous ammonium acetate, increased in average *m/z* from 1713.7732 to 1721.2884., by approximately 38 deuterons (Figure S-1). Calculating the increase in *m/z* upon in-trap HDX for the 11^+ is less straightforward, since the isolated 11^+ ions undergo both HDX with and proton transfer to ND_3, likely due to the reduced proton affinity of ubiquitin when additional excess charges are present.[48] Therefore, we are using the deuterated 10^+ ion formed by HDX and proton transfer to determine the extent of deuterium labeling (Figure S-2). The charge-deconvoluted average masses for non-deuterated ubiquitin 11^+ and deuterated/proton transfer product 10^+ were 8564.9958 and 8,624.8084 Da, indicating that on average approximately 60 deuteriums were incorporated. The significant increase in the extent of deuteration of the 11^+ charge state versus the lower charge state is consistent with previous studies and the fact that the 11^+ charge state presents a much more extended structure than the 6^+ and 5^+ ions originating from aqueous solutions.[39] ECD of the deuterium-exchanged ubiquitin 6^+ is exemplified by the zoomed-in fragment spectra of the c_6 non-deuterated and deuterated ions (Figure 2B). The non-deuterated c_6 ion displays a typical isotopic distribution of a small sequence ion. However, the weighted average of the deuterated c_6 ion isotopic distribution is 769.1309 *m/z*, showing, on average that five deuterons have been exchanged. The sequence of the ubiquitin c_6 ion is MQIFVK. Since gas-phase HDX with ND_3 is known to favor exchanging deuterons with hydrogens bound to side chain and termini heteroatoms over exchange with amide hydrogens,[33] we expect that maximum deuteration of rapidly exchanging sites would result in a total of 7 deuteriums exchanged (i.e., the two glutamine amide hydrogens, the two lysine amine hydrogens, the two N-terminal amine hydrogens, and the ionizing proton). In calculating the relative deuterium uptake (RDU) for ECD fragments, we have subtracted the contributions from ionizing protons/deuterons to facilitate comparing different length fragments (Equation 1). The five-deuteron increase indicates that for the c_6 ion, the relative deuterium exchange is 0.66.

$$RDU = \frac{Average\ Observed\ \frac{m}{z}\ Shift - z}{\#\ Rapid\ Exchange\ Sites - z} \qquad \text{Equation (1)}$$

Figure 3 details all c ions observed from three replicates of the fragmentation of ubiquitin 6^+. Overall, the number of deuteriums incorporated increased as fragment lengths increased. The increase in observed exchange for longer fragments correlates with the increase in the number of exchangeable hydrogens. Though the number of exchanges generally increases, there are several regions where exchange does not increase, indicating that fast-exchanging hydrogens are protected from exchange by either a lack of solvent accessibility or participation in hydrogen bonding.[5] For example, between residues 20 and 22 (SDT), the number of deuteriums does not increase, nor does the number of incorporated residues increase from residue 24 to 26 (ENV) All of these residues, other than valine, can undergo rapid exchange. This indicates that the extents of localized HDX are likely reporting on differences in accessibility and chemical microenvironment (i.e., structure).

It is also apparent that although ECD gives fragmentation throughout the protein's backbone, not every N-Cα bond is fragmented, making localized HDX for every residue impossible. Therefore, we interpreted our data such that the relative deuteration of regions of the protein are considered to localize the exchange data to obtain localized structural information. Since ECD fragmentation results capture of an electron by a nearby protonated residue[49] or facilitated by a nearby protonated residue,[50] we chose to end these regions with basic residues. As a result, these regions closely resemble tryptic fragments, allowing for HDX experiments with and without enzymatic cleavage to be readily compared. Thus, the following

results have reported relative deuterium exchange as a function of these pseudo tryptic fragments.

Localized HDX of Mobility Separated Conformers. During the HDX/IM/ECD workflow, ions are mass selected prior to HDX, separated by conformational families in the mobility cell, and then are fragmented following separation. Performing fragmentation after the IM separation results in fragments being aligned with the precursors' arrival times.[51] Using ECD without any additional collisional activation prevents scrambling upon fragmentation that can readily occur with CID.[39, 52-54] This workflow, with the ability to select charge states and separate conformers, allows for the localization of HDX for each conformational family that is kinetically trapped from the electrospray droplets.[24] An ion mobility separation of ubiquitin 6^+ in nitrogen typically results in the formation of a larger peak with an earlier arrival time and a smaller peak at longer arrival time.[55]

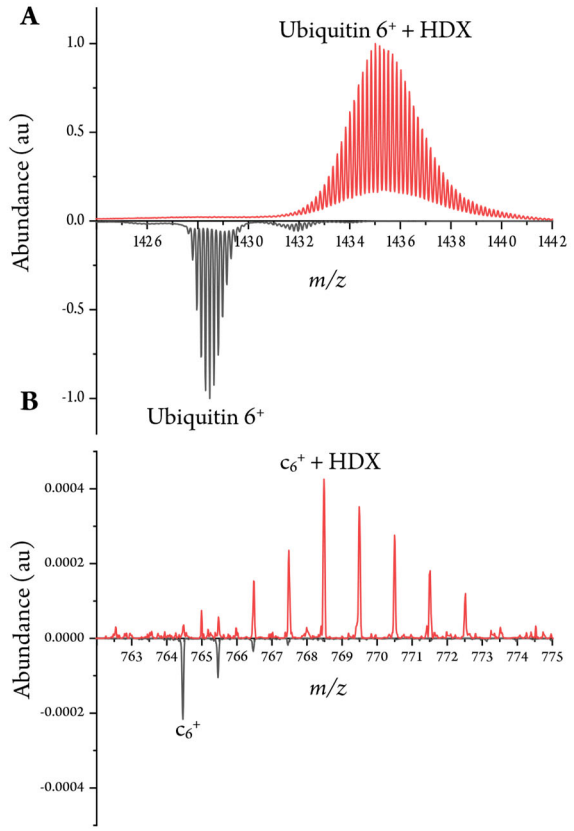

Figure 2. (A) Mass spectra of ubiquitin 6^+ with (red) and without (black) in-trap HDX. (B) Mass spectra of the ECD fragment c_6^+ with (red) and without (black) in-trap HDX.

By performing ECD after the mobility separation, localized HDX for each of these conformer families was observed (Figure 4). Figure 4A shows the arrival time distribution of the deuterated 6^+ ions. Extracting the ECD fragments for the earlier arriving peak, representing the more compact of the two major conformational families (I), shows that certain regions of the protein are more fully deuterated than other regions of the protein (Figure 4 B and D), evidence that the HDX/IMS/ECD experiments are indicative of localized changes in structure. For example, residues 7-11 showed a relative uptake of 0.67, while regions in the protein's interior showed relative deuteration more on the order of 0.4. Though it is not expected that every aspect of gas-phase protein structure is identical to solution, as the collapse of side chains in the gas-phase is known to occur,[56] comparisons of the gas-phase HDX data to condensed phase structures can aid in the interpretation of gas-phase structural information. The most protected regions of the protein were residues 12-33, which includes the main alpha helix, residues 43-48, a short turn region, and residues 55-63.[57] HDX results from the IM peak representing the most extended 6^+ conformer (II) are shown in Figure 4 C and E. The differences in relative deuterium uptake were plotted for cases where the average deuterium uptakes were significantly different as determined by a two-tailed t-test at an α value of 0.05. Interestingly, the greatest difference in uptake between the two conformers occurred in residues 43-48, the short turn region that was relatively protected against exchange in the more compact conformer. This indicates that this region is relatively dynamic for 6^+ ions. Since these structures are kinetically trapped and frozen on the timescale of the experiment,[24] they are separable by ion mobility, and thus, can be probed for localized differences in three-dimensional structure and dynamicity.

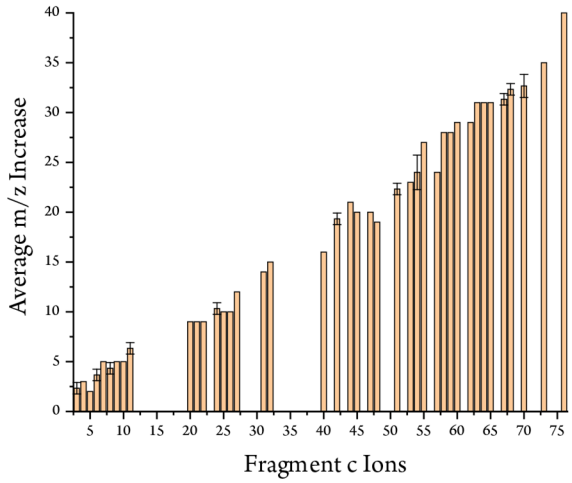

Figure 3. Plot of the weighted average *m/z* increase for c ion fragments from ubiquitin 6^+ after in-trap HDX. Error bars represent ± the standard deviation from three replicates.

HDX of more Compact and Extended Charge States. Nanoelectrospray of ubiquitin from ammonium acetate presents mainly the 5^+ and 6^+ charge states. Thus, we compared localized HDX between the most compact 6^+ conformer family and the 5^+ charge state. The arrival time distribution of the 5^+ charge state is found in Figure S-3. We only summed spectra between ~10 ms to 12 ms to reduce the impact of collisional heating on HD scrambling by avoiding analyzing data from the later arriving tail of the distribution. The results for the 5^+ charge state are shown comparatively in Figure 5. The majority of the protein sequence showed no significant change in deuteration between the 6^+ and the 5^+ structures, which is to be expected from kinetically trapped solution structures that maintain their overall fold in the gas phase. However, there were several regions that showed additional protection against deuteration for the 5^+ charge state. Residues 1-6, 34-42, and 64-76 showed greater protection against deuteration than for the compact 6^+ ions. This is likely due to the retention or gain of additional hydrogen bonds in the gas phase from reduced charge-charge repulsion of the 5^+ charge state versus the 6^+ charge state.[58-59] Additionally, due to the strong correlation

between solvent accessible surface area (SASA) and charge state,[27] these differences in HDX may be a result of small differences in the original solution structure.

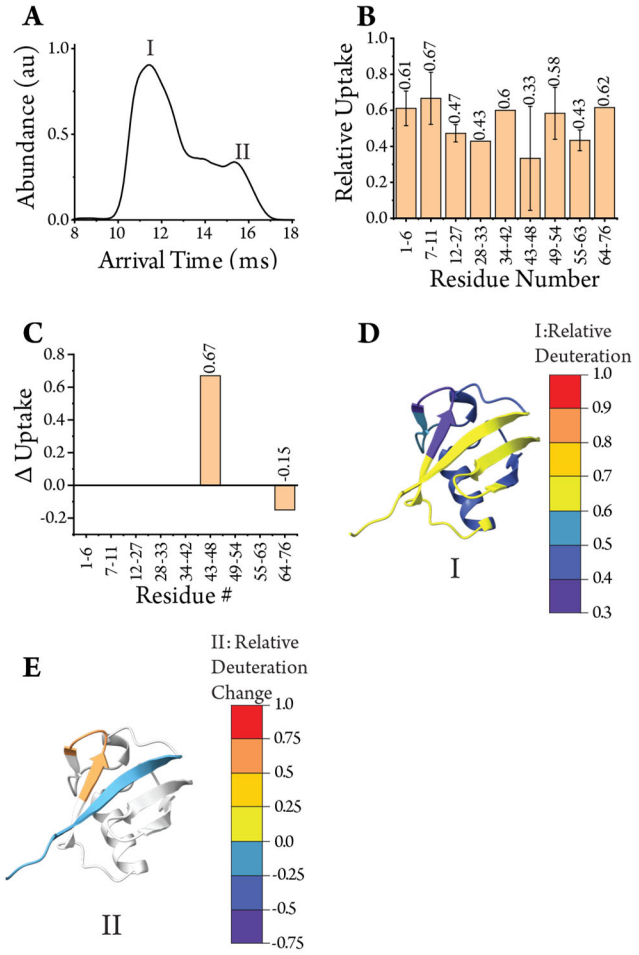

Figure 4. Differences in deuterium uptake between more compact and extended structures of ubiquitin 6^+. (A) Ion mobility spectrum of ubiquitin 6^+ from aqueous conditions following in-trap HDX. (B) Relative deuterium uptake for various sequence regions of the more compact 6^+ structure. Error bars represent standard deviations of triplicate measurements. (C) Difference in relative deuterium uptake between the more extended structure and the more compact structure for the same sequence regions. The significance of these differences was verified by t-tests at an α value of 0.05. (D) The compact structure (I) is color coded based upon the relative deuterium of various regions of the protein. (E) The more extended structure (II) is color coded based upon the increase or decrease in relative deuteration of the same regions with respect to the more compact structure.

The two main salt bridges in ubiquitin are between lysine 11 and glutamate 34, and lysine 27 and aspartate 52. The lack of a solvent system serves to strengthen salt bridges in the gas phase and salt bridges are expected to be the final structural motifs from solution that are lost.[60] ECD[32] and ultraviolet photodissociation (UVPD)[61] have been previously used to assign protonation sites of native-like ubiquitin structures. Notably, both ECD and UVPD showed that lysine 33 is protonated for the 6^+ ion, while UVPD and examination of ECD of the undeuterated 5^+ ions showed that lysine 33 was not protonated for the 5^+ ions, since the charge state of the fragments does not increase between z_{42}^{2+} and z_{45}^{2+} (i.e., between residues glycine 35 and lysine 29, respectively). Therefore, it is possible that protonation of the nearby lysine 33 destabilizes the salt bridge between lysine 11 and glutamate 34 and/or causes a different salt bridge to form. This might result in increased dynamicity for the 6^+ charge state. However, protonation states of lysine 63 and arginine 72/74 do not change between the two charge states, and there are no known salt bridges in this region. Nevertheless, this region is more protected for the 5^+ charge state than the 6^+ charge state, while residues 55-63 are less protected. The most likely explanation for differences in HDX between 5^+ and 6^+ charge states is that we are probing small differences in the more dynamic regions of the solution structures that are kinetically frozen in the gas phase.

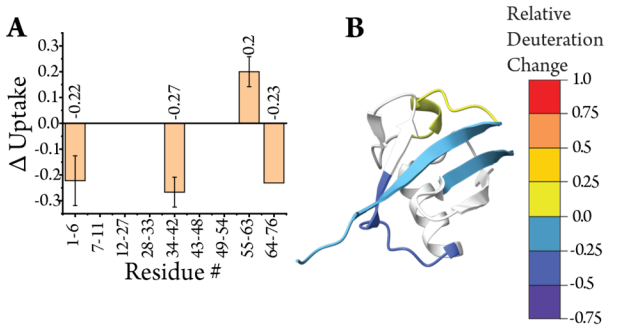

Figure 5. Differences in deuterium uptake between ubiquitin 5^+ and the compact ubiquitin 6^+ conformer. (A) Bar chart and (B) color coded structure representing the magnitude of the differences in relative deuterium uptake. The significance of these differences was verified by t-tests at a p value of 0.05.

Figure 6 shows the differences in relative exchange between the 6^+ native-like ions and the 11^+ ions formed from nESI from organic and acidic conditions. We expect that the 11^+ ions represent a kinetically trapped conformer that resembles the partially unfolded *A*-state of ubiquitin. The ATD of ubiquitin 11^+ shows mainly a single peak with a shoulder to the left of the distribution (Figure S-4 top). The post HDX distribution (S-4 bottom) shows several peaks, which is a result of proton transfer to deuterated ammonia from the protein. In this study, we used the ECD fragment spectra from the entire ATD, as the undeuterated ATD had only one major feature. However, if desired, these proton transfer product peaks could be eliminated by using a less basic deuterating reagent, such as deuterated methanol,[62-63] or the extent of the reaction could be reduced by varying the trap traveling wave, or by decreasing the partial pressure of ND_3 in the trap cell or the overall pressure in the cell.[38] By changing the reaction time, information about the HDX kinetics (i.e., structure) of different regions of the protein could be determined.

The *A*-state is characterized by loss of the native structure in the C-terminal half of the protein into an extended coiled form.[64] As a result, it is expected that the C-terminal region would undergo more rapid exchange than for the native state, since the side chains in the C-terminal half are no longer buried in the core of the protein. A model of the *A*-state constrained by NMR measurements[64-65] has illustrated that residue 39 to residue 72 form a single extended alpha helix, and salt bridges that stabilize the native state are disrupted. We observed significant increases in exchange throughout the protein, especially for regions such as the main α helix that are well protected

against exchange in the native-like structures, indicative of a partially unfolded structure.

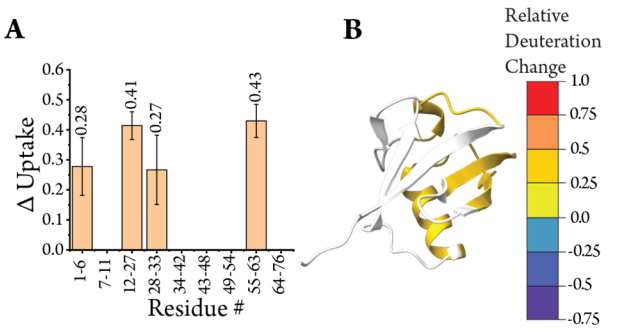

Figure 6. Differences in deuterium uptake between ubiquitin 11^+ and the compact ubiquitin 6^+ conformer. (A) Bar chart and (B) color coded structure representing the magnitude of the differences in relative deuterium uptake. The significance of these differences was verified by t-tests at a p value of 0.05.

HDX of Native-Like Cytochrome C. As an additional model case, the most abundant charge state of cytochrome c resulting from nESI from an ammonium acetate solution, the 7^+ charge state, was isolated and allowed to exchange with ND_3 in the trap cell. Again, ECD was used to localize the exchange data. The ATD of cytochrome c 7^+ is mainly a single feature; we did not incorporate the data for the minor peak at longer arrival time (Figure S-5) in our data analysis. Figure 7 shows the relative deuterium uptake of different regions of cytochrome c upon gas-phase HDX. The following trends were observed. First, in general, more structured regions of the protein, for instance, alpha helical regions and regions proximal to heme binding, as determined by the crystal structure (Figure 7B),[66] showed a moderate level of exchange. However, more disordered loop sections of the protein and the helical regions farther from the heme showed additional exchange. For example, the disordered region comprised of residues 23-35 showed a relative deuterium exchange of 1.4, indicating that all exchangeable side chain hydrogens and some amide backbone hydrogens were exchanged. These data correlate with the conservation of important aspects of solution structure in the gas phase and show the ability of gas-phase HDX-IM-ECD to provide localized structural information.

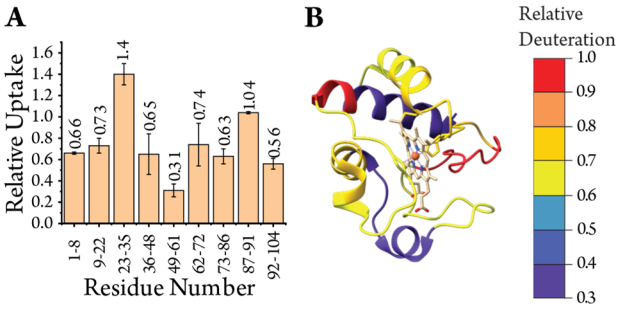

Figure 7. Relative deuterium uptake for cytochrome c 7^+ (A) Bar chart and (B) color coded structure representing the magnitude of the relative deuterium uptake.

CONCLUSIONS

In this article, we have shown the application of ion mobility and transmission-mode ECD to gas-phase HDX. Our results appear to show that by avoiding collisional activation, this method provides for localized three-dimensional structural information of gaseous protein ions. Exchange information for protein ions formed by nESI from aqueous conditions shows that regions of the proteins whose side chains are expected to be more protected against exchange based on their condensed phase structures are indeed more protected in the gas phase. In contrast, more unstructured regions of the protein and side chains that are closer to the surface of the protein exchanged more completely. Equilibrium gas-phase structures of native like proteins give an "inside-out" orientation, with the hydrophobic interior being refolded to the surface of the protein and the external, more hydrophilic portion towards the interior.[67] Therefore, our results, along with of other gas-phase evidence, suggest that kinetically trapped solution-like states are preserved over a typical MS timescale and that inside-out gas-phase equilibrium structures are not populated. The application of a mobility separation prior to ECD allows HDX to be determined as a function of conformational family, a key aspect of this workflow versus workflows that employ fragmentation prior to mobility separation, perform HDX in the mobility cell itself, require post-mobility trapping, or do not have ion mobility. This allowed us to separate more compact and extended conformers of the 6^+ charge state of ubiquitin, with HDX illuminating significant differences between the two gas-phase structures. Finally, localized HDX for the partially folded *A*-state of ubiquitin, measured utilizing the 11^+ charge state, showed greater exchange throughout the entire protein, as is expected following the loss of structurally stabilizing salt bridges.

Future efforts for this workflow will include developing the ability to use different exchange conditions to generate HDX kinetics data. The number of collisions that ions experience with ND_3 or other exchange reagent gases can be controlled by changing the partial pressure of ND_3, the background gas pressure of the cell, or the trap traveling wave velocity and height.[38] These changes in collision rates and labeling times would allow exchange kinetics to be probed, giving much more detailed structural information. Another advantage of controlling exchange rates would be to minimize charge reduction reactions of higher charged protein ions, which can complicate the mobility spectra due the charge dependence on ion mobility. Furthermore, the identity of the reagent gas could be changed to a less basic reagent. However, the mechanism of gas-phase HDX is known to change with the proton affinity of the reagent,[62] so care must be taken in the interpretation of results with different reagent gases. In sum, we expect that HDX-IM-ECD will be a useful tool for characterizing gaseous protein structures, especially for dynamic systems that are difficult to characterize with condensed phase methods.

ASSOCIATED CONTENT

Supporting Information

(1) Mass spectra of ubiquitin 5^+ before and after gas-phase HDX, (2) mass spectra of ubiquitin 11^+ before and 10^+ after gas-phase HDX, (3) arrival time distribution of deuterated ubiquitin 5^+, (4) arrival time distribution of undeuterated ubiquitin 11^+ and the products of gas-phase deuterated 11^+, (5) arrival time distribution of deuterated cytochrome c

7^{+}. The Supporting Information is available free of charge on the ACS Publications website.

Corresponding Author

* ikwebb@iu.edu

Author Contributions

The manuscript was written through contributions of all authors. / All authors have given approval to the final version of the manuscript. /

ACKNOWLEDGMENT

Portions of this work were funded by the Indiana University Purdue University Indianapolis School of Science (Startup Funds, I.K.W.) and an American Society for Mass Spectrometry Research Award (I.K.W.). We would also like to acknowledge Dr. Ulrik Mistarz and Professor Kasper Rand for helpful discussions.

REFERENCES

1. Fenn, J. B., Electrospray wings for molecular elephants (Nobel lecture). *Angew Chem Int Ed Engl* **2003,** *42* (33), 3871-94.
2. Chait, B. T.; Cadene, M.; Olinares, P. D.; Rout, M. P.; Shi, Y., Revealing Higher Order Protein Structure Using Mass Spectrometry. *J Am Soc Mass Spectrom* **2016,** *27* (6), 952-965.
3. Limpikirati, P.; Liu, T.; Vachet, R. W., Covalent labeling-mass spectrometry with non-specific reagents for studying protein structure and interactions. *Methods* **2018,** *144*, 79-93.
4. Mendoza, V. L.; Vachet, R. W., Probing protein structure by amino acid-specific covalent labeling and mass spectrometry. *Mass Spectrom Rev* **2009,** *28* (5), 785-815.
5. Englander, S. W., Hydrogen exchange and mass spectrometry: A historical perspective. *J Am Soc Mass Spectrom* **2006,** *17* (11), 1481-1489.
6. Chavez, J. D.; Wippel, H. H.; Tang, X.; Keller, A.; Bruce, J. E., In-Cell Labeling and Mass Spectrometry for Systems-Level Structural Biology. *Chemical Reviews* **2021**.
7. Novak, P.; Kruppa, G. H.; Young, M. M.; Schoeniger, J., A top-down method for the determination of residue-specific solvent accessibility in proteins. *J Mass Spectrom* **2004,** *39* (3), 322-8.
8. Sinz, A., Chemical cross-linking and mass spectrometry to map three-dimensional protein structures and protein-protein interactions. *Mass Spectrom Rev* **2006,** *25* (4), 663-82.
9. Manzi, L.; Barrow, A. S.; Scott, D.; Layfield, R.; Wright, T. G.; Moses, J. E.; Oldham, N. J., Carbene footprinting accurately maps binding sites in protein–ligand and protein–protein interactions. *Nature Communications* **2016,** *7* (1), 13288.
10. Vahidi, S.; Stocks, B. B.; Liaghati-Mobarhan, Y.; Konermann, L., Mapping pH-induced protein structural changes under equilibrium conditions by pulsed oxidative labeling and mass spectrometry. *Anal Chem* **2012,** *84* (21), 9124-30.
11. Li, K. S.; Shi, L.; Gross, M. L., Mass Spectrometry-Based Fast Photochemical Oxidation of Proteins (FPOP) for Higher Order Structure Characterization. *Acc Chem Res* **2018,** *51* (3), 736-744.
12. Zhang, Y.; Fonslow, B. R.; Shan, B.; Baek, M. C.; Yates, J. R., 3rd, Protein analysis by shotgun/bottom-up proteomics. *Chem Rev* **2013,** *113* (4), 2343-94.
13. Masson, G. R.; Burke, J. E.; Ahn, N. G.; Anand, G. S.; Borchers, C.; Brier, S.; Bou-Assaf, G. M.; Engen, J. R.; Englander, S. W.; Faber, J.; Garlish, R.; Griffin, P. R.; Gross, M. L.; Guttman, M.; Hamuro, Y.; Heck, A. J. R.; Houde, D.; Iacob, R. E.; Jorgensen, T. J. D.; Kaltashov, I. A.; Klinman, J. P.; Konermann, L.; Man, P.; Mayne, L.; Pascal, B. D.; Reichmann, D.; Skehel, M.; Snijder, J.; Strutzenberg, T. S.; Underbakke, E. S.; Wagner, C.; Wales, T. E.; Walters, B. T.; Weis, D. D.; Wilson, D. J.; Wintrode, P. L.; Zhang, Z.; Zheng, J.; Schriemer, D. C.; Rand, K. D., Recommendations for performing, interpreting and reporting hydrogen deuterium exchange mass spectrometry (HDX-MS) experiments. *Nat Methods* **2019,** *16* (7), 595-602.
14. Jørgensen, T. J. D.; Gårdsvoll, H.; Ploug, M.; Roepstorff, P., Intramolecular Migration of Amide Hydrogens in Protonated Peptides upon Collisional Activation. *Journal of the American Chemical Society* **2005,** *127* (8), 2785-2793.
15. Brown, K. A.; Wilson, D. J., Bottom-up hydrogen deuterium exchange mass spectrometry: data analysis and interpretation. *Analyst* **2017,** *142* (16), 2874-2886.
16. Mendoza, V. L.; Vachet, R. W., Protein surface mapping using diethylpyrocarbonate with mass spectrometric detection. *Anal Chem* **2008,** *80* (8), 2895-904.
17. Leney, A. C.; Heck, A. J. R., Native Mass Spectrometry: What is in the Name? *J Am Soc Mass Spectrom* **2017,** *28* (1), 5-13.
18. Webb, I. K., Recent technological developments for native mass spectrometry. *Biochimica et Biophysica Acta (BBA) - Proteins and Proteomics* **2022,** *1870* (1), 140732.
19. Konijnenberg, A.; Butterer, A.; Sobott, F., Native ion mobility-mass spectrometry and related methods in structural biology. *Biochim Biophys Acta* **2013,** *1834* (6), 1239-56.
20. Ruotolo, B. T.; Giles, K.; Campuzano, I.; Sandercock, A. M.; Bateman, R. H.; Robinson, C. V., Evidence for macromolecular protein rings in the absence of bulk water. *Science* **2005,** *310* (5754), 1658-61.
21. Schmidt, C.; Robinson, C. V., Dynamic protein ligand interactions--insights from MS. *FEBS J* **2014,** *281* (8), 1950-64.
22. Tian, Y.; Han, L.; Buckner, A. C.; Ruotolo, B. T., Collision Induced Unfolding of Intact Antibodies: Rapid Characterization of Disulfide Bonding Patterns, Glycosylation, and Structures. *Anal Chem* **2015,** *87* (22), 11509-15.
23. Keener, J. E.; Zhang, G.; Marty, M. T., Native Mass Spectrometry of Membrane Proteins. *Anal Chem* **2021,** *93* (1), 583-597.
24. Raab, S. A.; El-Baba, T. J.; Laganowsky, A.; Russell, D. H.; Valentine, S. J.; Clemmer, D. E., Protons Are Fast and Smart; Proteins Are Slow and Dumb: On the Relationship of Electrospray Ionization Charge States and Conformations. *J Am Soc Mass Spectrom* **2021,** *32* (7), 1553-1561.
25. Revercomb, H. E.; Mason, E. A., Theory of plasma chromatography/gaseous electrophoresis. Review. *Analytical Chemistry* **2002,** *47* (7), 970-983.
26. Ruotolo, B. T.; Benesch, J. L.; Sandercock, A. M.; Hyung, S. J.; Robinson, C. V., Ion mobility-mass spectrometry analysis of large protein complexes. *Nat Protoc* **2008,** *3* (7), 1139-52.
27. Testa, L.; Brocca, S.; Grandori, R., Charge-Surface Correlation in Electrospray Ionization of Folded and Unfolded Proteins. *Analytical Chemistry* **2011,** *83* (17), 6459-6463.
28. Allison, T. M.; Landreh, M., Chapter Six - Ion Mobility in Structural Biology. In *Comprehensive Analytical Chemistry*, Donald, W. A.; Prell, J. S., Eds. Elsevier: 2019; Vol. 83, pp 161-195.
29. Webb, I. K.; Morrison, L. J.; Brown, J., Dueling electrospray implemented on a traveling-wave ion mobility/time-of-flight mass spectrometer: Towards a gas-phase workbench for structural biology. *International Journal of Mass Spectrometry* **2019,** *444*, 116177.
30. Carvalho, V. V.; See Kit, M. C.; Webb, I. K., Ion Mobility and Gas-Phase Covalent Labeling Study of the Structure and Reactivity of Gaseous Ubiquitin Ions Electrosprayed from Aqueous and Denaturing Solutions. *J Am Soc Mass Spectrom* **2020,** *31* (5), 1037-1046.
31. Cheung See Kit, M.; Shepherd, S. O.; Prell, J. S.; Webb, I. K., Experimental Determination of Activation Energies for Covalent Bond Formation via Ion/Ion Reactions and Competing Processes. *J Am Soc Mass Spectrom* **2021,** *32* (9), 2313-2321.
32. Cheung See Kit, M.; Carvalho, V. V.; Vilseck, J. Z.; Webb, I. K., Gas-Phase Ion/Ion Chemistry for Structurally Sensitive Probes of Gaseous Protein Ion Structure: Electrostatic and Electrostatic to Covalent Cross-Linking. *Int J Mass Spectrom* **2021,** *463*, 116549.
33. Cheng, X.; Fenselau, C., Hydrogen/deuterium exchange of mass-selected peptide ions with ND3 in a tandem sector mass spectrometer. *International Journal of Mass Spectrometry and Ion Processes* **1992,** *122*, 109-119.
34. Suckau, D.; Shi, Y.; Beu, S. C.; Senko, M. W.; Quinn, J. P.; Wampler, F. M.; McLafferty, F. W., Coexisting stable conformations of gaseous protein ions. *Proceedings of the National Academy of Sciences* **1993,** *90* (3), 790.
35. Mao, D.; Douglas, D. J., H/D exchange of gas phase bradykinin ions in a linear quadrupole ion trap. *J Am Soc Mass Spectrom* **2003,** *14* (2), 85-94.
36. Kaltashov, I. A.; Doroshenko, V. M.; Cotter, R. J., Gas phase hydrogen/deuterium exchange reactions of peptide ions in a quadrupole ion trap mass spectrometer. *Proteins: Structure, Function, and Bioinformatics* **1997,** *28* (1), 53-58.

37. Valentine, S. J.; Clemmer, D. E., H/D Exchange Levels of Shape-Resolved Cytochrome c Conformers in the Gas Phase. *Journal of the American Chemical Society* **1997,** *119* (15), 3558-3566.
38. Rand, K. D.; Pringle, S. D.; Murphy, J. P., 3rd; Fadgen, K. E.; Brown, J.; Engen, J. R., Gas-phase hydrogen/deuterium exchange in a traveling wave ion guide for the examination of protein conformations. *Anal Chem* **2009,** *81* (24), 10019-28.
39. Rand, K. D.; Pringle, S. D.; Morris, M.; Brown, J. M., Site-specific analysis of gas-phase hydrogen/deuterium exchange of peptides and proteins by electron transfer dissociation. *Anal Chem* **2012,** *84* (4), 1931-40.
40. Rand, K. D.; Adams, C. M.; Zubarev, R. A.; Jørgensen, T. J. D., Electron Capture Dissociation Proceeds with a Low Degree of Intramolecular Migration of Peptide Amide Hydrogens. *Journal of the American Chemical Society* **2008,** *130* (4), 1341-1349.
41. Khakinejad, M.; Kondalaji, S. G.; Maleki, H.; Arndt, J. R.; Donohoe, G. C.; Valentine, S. J., Combining Ion Mobility Spectrometry with Hydrogen-Deuterium Exchange and Top-Down MS for Peptide Ion Structure Analysis. *J Am Soc Mass Spectrom* **2014,** *25* (12), 2103-2115.
42. Williams, J. P.; Morrison, L. J.; Brown, J. M.; Beckman, J. S.; Voinov, V. G.; Lermyte, F., Top-Down Characterization of Denatured Proteins and Native Protein Complexes Using Electron Capture Dissociation Implemented within a Modified Ion Mobility-Mass Spectrometer. *Anal Chem* **2020,** *92* (5), 3674-3681.
43. Hoaglund, C. S.; Valentine, S. J.; Sporleder, C. R.; Reilly, J. P.; Clemmer, D. E., Three-dimensional ion mobility/TOFMS analysis of electrosprayed biomolecules. *Anal Chem* **1998,** *70* (11), 2236-42.
44. Wyttenbach, T.; Bowers, M. T., Structural stability from solution to the gas phase: native solution structure of ubiquitin survives analysis in a solvent-free ion mobility-mass spectrometry environment. *J Phys Chem B* **2011,** *115* (42), 12266-75.
45. Mistarz, U. H.; Rand, K. D., Installation, validation, and application examples of two instrumental setups for gas-phase HDX-MS analysis of peptides and proteins. *Methods* **2018,** *144*, 113-124.
46. Sanguantrakun, N.; Chanthamontri, C.; Gross, M. L., Top-Down Analysis of In-Source HDX of Native Protein Ions. *J Am Soc Mass Spectrom* **2020,** *31* (5), 1151-1154.
47. Kostyukevich, Y.; Kononikhin, A.; Popov, I.; Nikolaev, E., Conformational changes of ubiquitin during electrospray ionization as determined by in-ESI source H/D exchange combined with high-resolution MS and ECD fragmentation. *Journal of Mass Spectrometry* **2014,** *49* (10), 989-994.
48. Cassady, C. J.; Wronka, J.; Kruppa, G. H.; Laukien, F. H.; Hettich, R., Deprotonation reactions of multiply protonated ubiquitin ions. *Rapid Communications in Mass Spectrometry* **1994,** *8* (5), 394-400.
49. Breuker, K.; Oh, H.; Lin, C.; Carpenter, B. K.; McLafferty, F. W., Nonergodic and conformational control of the electron capture dissociation of protein cations. *Proc Natl Acad Sci U S A* **2004,** *101* (39), 14011-14016.
50. Tureček, F.; Chen, X.; Hao, C., Where Does the Electron Go? Electron Distribution and Reactivity of Peptide Cation Radicals Formed by Electron Transfer in the Gas phase. *Journal of the American Chemical Society* **2008,** *130* (27), 8818-8833.
51. Valentine, S. J.; Koeniger, S. L.; Clemmer, D. E., A Split-Field Drift Tube for Separation and Efficient Fragmentation of Biomolecular Ions. *Analytical Chemistry* **2003,** *75* (22), 6202-6208.
52. Pan, J.; Han, J.; Borchers, C. H.; Konermann, L., Hydrogen/deuterium exchange mass spectrometry with top-down electron capture dissociation for characterizing structural transitions of a 17 kDa protein. *J Am Chem Soc* **2009,** *131* (35), 12801-8.
53. Abzalimov, R. R.; Kaltashov, I. A., Controlling hydrogen scrambling in multiply charged protein ions during collisional activation: implications for top-down hydrogen/deuterium exchange MS utilizing collisional activation in the gas phase. *Anal Chem* **2010,** *82* (3), 942-50.
54. Wollenberg, D. T. W.; Pengelley, S.; Mouritsen, J. C.; Suckau, D.; Jorgensen, C. I.; Jorgensen, T. J. D., Avoiding H/D Scrambling with Minimal Ion Transmission Loss for HDX-MS/MS-ETD Analysis on a High-Resolution Q-TOF Mass Spectrometer. *Anal Chem* **2020,** *92* (11), 7453-7461.
55. May, J. C.; Jurneczko, E.; Stow, S. M.; Kratochvil, I.; Kalkhof, S.; McLean, J. A., Conformational Landscapes of Ubiquitin, Cytochrome c, and Myoglobin: Uniform Field Ion Mobility Measurements in Helium and Nitrogen Drift Gas. *Int J Mass Spectrom* **2018,** *427*, 79-90.
56. Bakhtiari, M.; Konermann, L., Protein Ions Generated by Native Electrospray Ionization: Comparison of Gas Phase, Solution, and Crystal Structures. *J Phys Chem B* **2019,** *123* (8), 1784-1796.
57. Vijay-kumar, S.; Bugg, C. E.; Cook, W. J., Structure of ubiquitin refined at 1.8 Å resolution. *Journal of Molecular Biology* **1987,** *194* (3), 531-544.
58. Breuker, K.; McLafferty, F. W., Stepwise evolution of protein native structure with electrospray into the gas phase, 10(-12) to 10(2) s. *Proc Natl Acad Sci U S A* **2008,** *105* (47), 18145-52.
59. Breuker, K.; Oh, H.; Horn, D. M.; Cerda, B. A.; McLafferty, F. W., Detailed unfolding and folding of gaseous ubiquitin ions characterized by electron capture dissociation. *J Am Chem Soc* **2002,** *124* (22), 6407-20.
60. Skinner, O. S.; McLafferty, F. W.; Breuker, K., How ubiquitin unfolds after transfer into the gas phase. *J Am Soc Mass Spectrom* **2012,** *23* (6), 1011-4.
61. Morrison, L. J.; Brodbelt, J. S., Charge site assignment in native proteins by ultraviolet photodissociation (UVPD) mass spectrometry. *Analyst* **2016,** *141* (1), 166-76.
62. Campbell, S.; Rodgers, M. T.; Marzluff, E. M.; Beauchamp, J. L., Deuterium Exchange Reactions as a Probe of Biomolecule Structure. Fundamental Studies of Gas Phase H/D Exchange Reactions of Protonated Glycine Oligomers with D2O, CD3OD, CD3CO2D, and ND3. *Journal of the American Chemical Society* **1995,** *117* (51), 12840-12854.
63. Mistarz, U. H.; Brown, J. M.; Haselmann, K. F.; Rand, K. D., Simple setup for gas-phase H/D exchange mass spectrometry coupled to electron transfer dissociation and ion mobility for analysis of polypeptide structure on a liquid chromatographic time scale. *Anal Chem* **2014,** *86* (23), 11868-76.
64. Harding, M. M.; Williams, D. H.; Woolfson, D. N., Characterization of a partially denatured state of a protein by two-dimensional NMR: reduction of the hydrophobic interactions in ubiquitin. *Biochemistry* **1991,** *30* (12), 3120-8.
65. Brutscher, B.; Brüschweiler, R.; Ernst, R. R., Backbone Dynamics and Structural Characterization of the Partially Folded A State of Ubiquitin by 1H, 13C, and 15N Nuclear Magnetic Resonance Spectroscopy. *Biochemistry* **1997,** *36* (42), 13043-13053.
66. Bushnell, G. W.; Louie, G. V.; Brayer, G. D., High-resolution three-dimensional structure of horse heart cytochrome c. *J Mol Biol* **1990,** *214* (2), 585-95.
67. Sever, A. I. M.; Konermann, L., Gas Phase Protein Folding Triggered by Proton Stripping Generates Inside-Out Structures: A Molecular Dynamics Simulation Study. *J Phys Chem B* **2020,** *124* (18), 3667-3677.